AEROELASTIC WIND TUNNEL EXPERIMENT OF A HIGH-ASPECT-RATIO WING MODEL AGAINST GEOMETRICAL NON-LINEARITY

Wei Qian*, Yuguang Bai*, Huihua Zeng, Rui Yang*****
***School of Aeronautics and Astronautics, Dalian University of Technology, Dalian 116023, China; **Shenyang Aircraft Design Institute, Shenyang 110035, China; ***School of Mechanical Engineering, Dalian University of Technology, Dalian 116023, China**

Keywords: *high-aspect-ratio wing; aeroelastic; wind tunnel experiment; geometrical non-linearity*

Abstract

Geometrical non-linearity due to static deformation of high-aspect-ratio wing is closely related to aeroelastic characteristics. Generally, a small deformation is corresponding to a basic flutter mode while another different aeroelastic phenomenon can be observed due to large deformation. Many existed studies have presented this pattern. A high-aspect-ratio wing model was designed and manufactured to investigate this kind of flutter patterns. Flutter wind tunnel experiments was finished with FL-26 wind tunnel in China. Also, a nonlinear FEM numerical method was employed to study the effect of large deformation on the flutter characteristics of the present high-aspect-ratio wind model, which was associated with the experimental results. The investigated results provided the process on the reveal of aeroelastic characteristics of high-aspect-ratio wing with large deformation, which will also be useful for some other novel numerical method and experimental model design.

1 Introduction

As an important step for commercial aircraft design, analysis of high-aspect-ratio wings with numerical simulations and wind tunnel experiments are necessary. It was difficult to simulate elastic characteristic due to nonlinear deformation of a high-aspect-ratio wing.

Lu et al.[1] identified the aeroelastic responses of a high-aspect-ratio flexible wing model and investigate the active flutter suppression for it using a trailing edge control surface, and they found that the present active control system could suppress the flutter at the optimized gain and phase delay. Hewson et al.[2] employed CFD method based on URANS modelling to investigate separated flow on high-aspect-ratio flexible wings, it proposed how to the process of determine semi-empirical coefficients for three dynamic stall models. Castellani et al.[3] developed two procedures for the nonlinear static aeroelastic analysis of flexible high-aspect-ratio wing aircraft subject to geometric nonlinearities, significant differences are found between linear and nonlinear approaches. Most studies proposed that nonlinear aeroelastic analysis must be taken during the design process of the related aircraft.

The present work wanted to study different flutter characteristics of high-aspect-ratio wing with large deformation which can bring geometrical non-linearity effects. Both wind tunnel tests and numerical method were employed. Through the experimental phenomenon, a series of new flutter characteristics were observed. With numerical studies, some aeroelastic pattern can be analyzed.

2 Design of the present experimental model

The experimental parameters were mainly chosen as: Mach number was 0.6 and dynamic pressure was 30Kpa. A half-model was chosen based on the parameters of FL-26 wind tunnel in

China, as shown in Fig.1 and Fig.2. Then an actual model was manufactured as Fig.3.

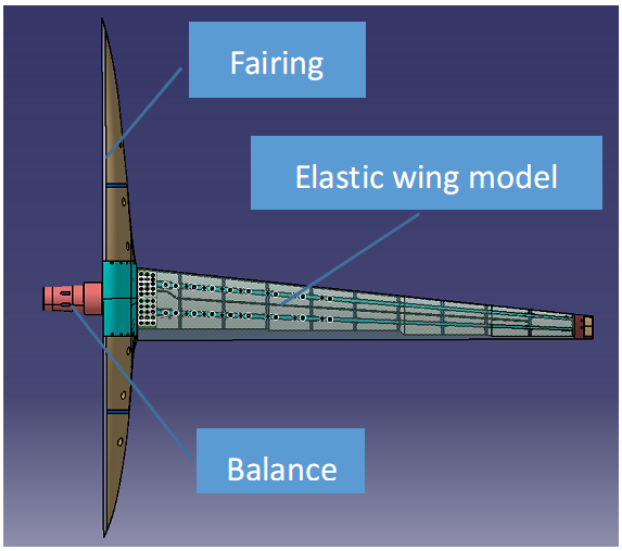

Fig.1 Design of the experimental model.

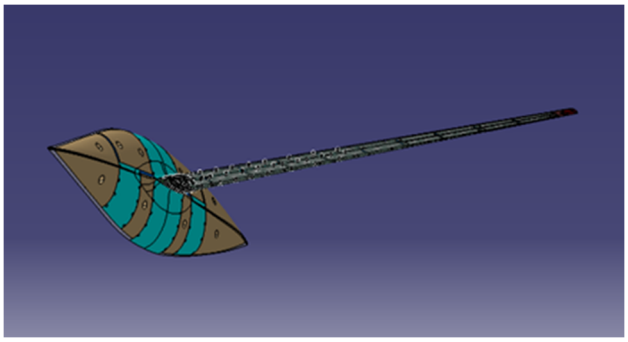

Fig.2 Model for manufacture.

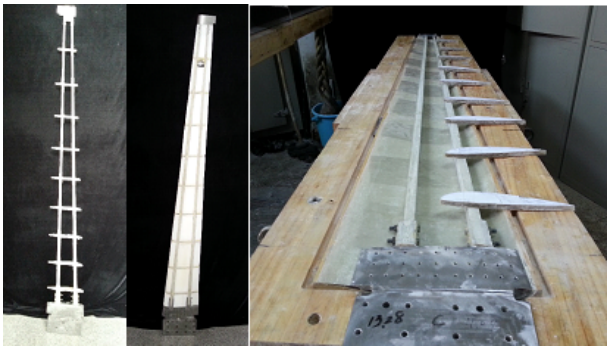

Fig.3 Manufacture of the experimental mode.

The elastic wing model was supported on the balance of the side wall of the wind tunnel. The fairing can be mounted on the rotating disc related to structure of the angle of attack, but it was not connected with the wing directly. This mean that it did not affect the measurement of the frequency and balance of the wing.

The wing model consists of steel joints and FRP structures, including skins, beams and ribs and PMI foams in the wing. The entire elastic wing is finally molded in the mold, as shown in Fig. 3.

3 Numerical simulations

3.1 FEM modelling

A FEM simulation model is established for the elastic model structure of the present high-aspect-ratio wing, as shown in Fig.4. Based on this model, modes of the wing were calculated and plotted in Fig,5. Also flutter characteristic calculation in the rear section also employed this model.

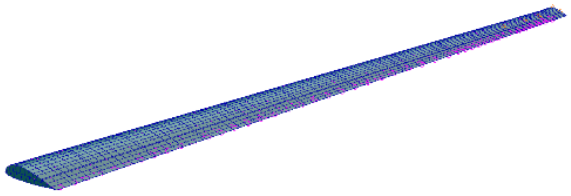

Fig.4 FEM modelling of the present wing.

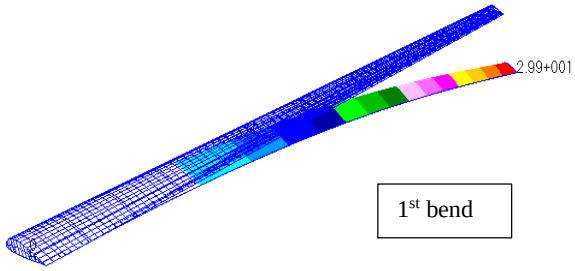

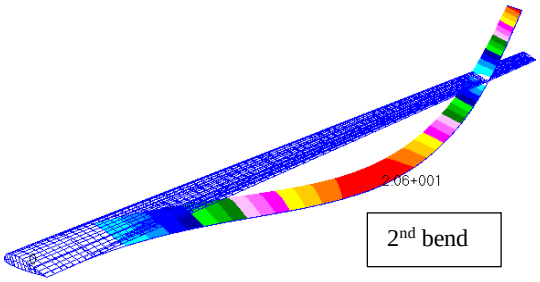

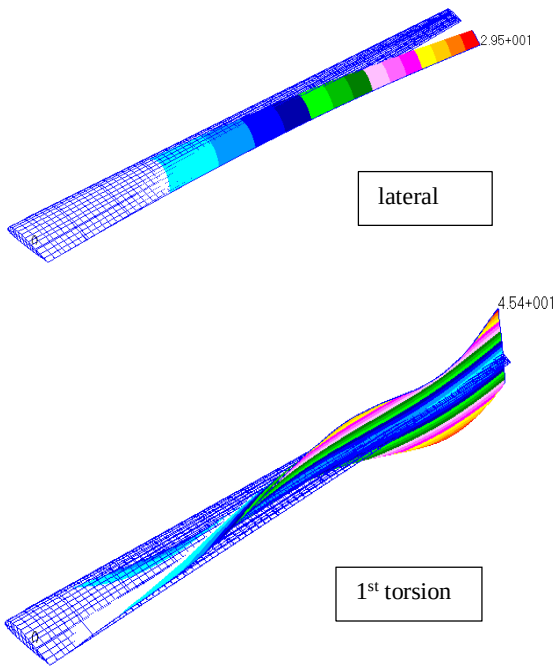

Fig.5 Typical modes of the present wing.

3.2 Flutter calculation

A flow chart was proposed in order to capture the geometric nonlinear effects caused by large deformation when taking the calculation of flutter, shown in Fig. 6. Firstly, the constant aerodynamic load is calculated when a certain angle of attack was set; secondly, the elastic deformation was calculated, the nonlinear algorithm with MARC is used to iterate the aerodynamic load until it converged to the equilibrium state when the frequency and mode of the model were calculated; Then the Double Lattice method was adopted to calculate the flutter boundary, which was obtained for the next change of the angle of attack. Computation was performed until all the flutter boundaries of the desired attack state were calculated.

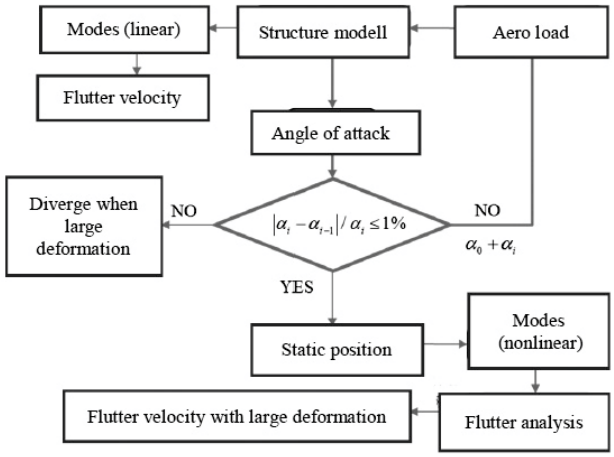

Fig.6 Flow chart of numerical simulation.

4 Model experiments

4.1 Flexibility test

Before the beginning of the wind tunnel test, the flexibility influence coefficient was firstly measured. Flexibility influence coefficients of the 22 control point was measured by the special loading and displacement measuring equipment, as shown in Fig.7.

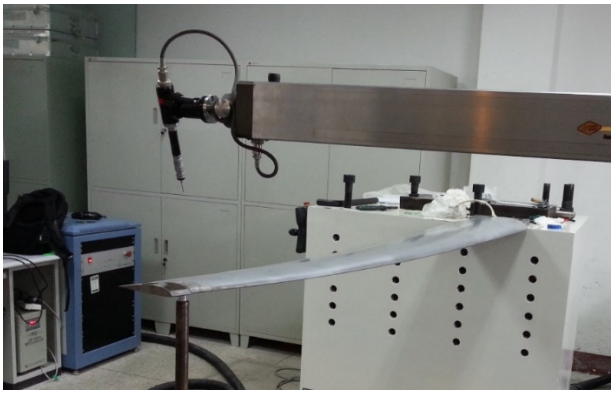

Fig.7 Flexibility test.

4.2 GVT experiments

Frequency experiment was finished [illegible] Siemens LMS Test.Lab system, a[illegible] Fig.8; the exciting force hammer used was produced by the Jiangsu Lianneng corporation in China, as shown in Fig.9; and the acceleration transducer used was ICP Piezoelectric acceleration transducer by PCB corporation. Experimental modes from LMS test system was shown in Fig.10 and Table 1.

Aero load

Fig.8 Siemens LMS Test.lib system.

Fig.9 Exciting force hammer.

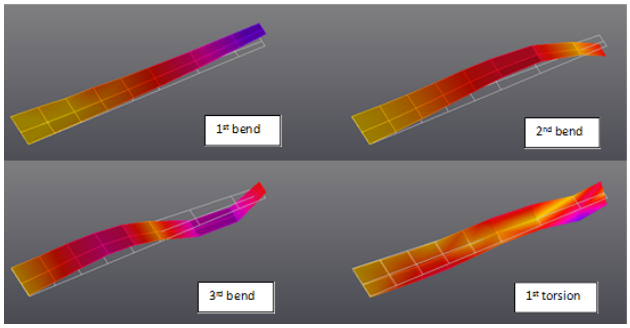

Fig.10 Modes from GVT experiments.

Table 1 GVT results

Mode	1st bend	2nd bend	3rd bend	1st torsion	lateral
Frequency (Hz)	6.23	24.81	61.69	105.11	34.98
Damping (%)	0.51	0.37	0.47	0.67	—

5 Wind tunnel test

The installation of the model in the wind tunnel is shown in Fig.11. The accelerometers in both horizontal and vertical directions were placed in the model to measure the vibration response of the model for two directions. The steps of the flutter wind tunnel test were shown in Fig.12. Under Ma=0.6 conditions, the wind tunnel holds an angle of attack every test when the velocity pressure was increased. It was seen that whether the flutter could occur. Then the angle of attack was change to carry out the next test. A typical acceleration response at the occurrence of the flutter was shown in Fig.13.

Fig.11 Model arrangement in the wind tunnel.

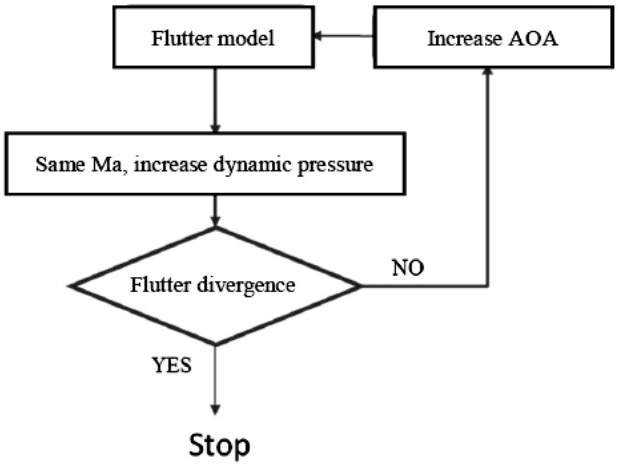

Fig.12 Steps of wind tunnel test.

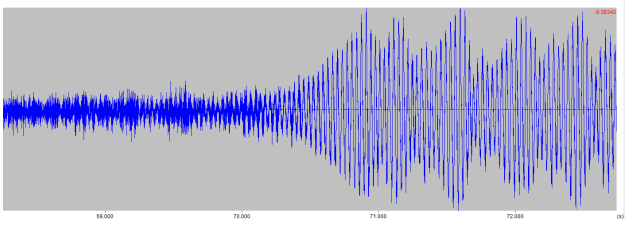

Fig.13 A typical acceleration response of flutter.

The wing deformation was measured by the binocular VMD measurement system which was installed on the upper panel of the experimental section. The deformation of each target point on

the wing model were obtained through software data processing. The identification of the VMD measurement points on the model was shown in Fig.14, and the schematic diagram of the basic principle of VMD was shown in Fig.15.

Fig.14 VMD points in the wind model

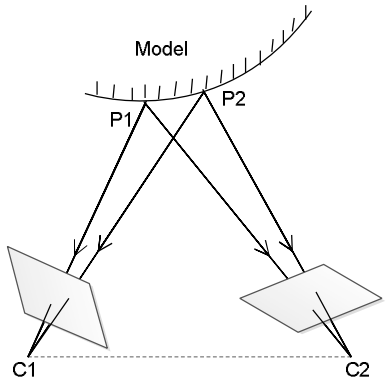

Fig.15 Schematic diagram of VMD testing system.

6 Discussion and conclusion

With Ma=0.6, four angles of attack -1°, -2°, -3°, -4° are adopted for wind tunnel tests. Because the wing was an asymmetric airfoil with high lifting force, the zero lifting angle of attack was approximately at -2°, so the wing was deformed to both sides at different angles of attack, as the result of deformation measurements shown in Fig.16 and Fig.17. Wind tunnel test results of flutter were shown in Table 2.

It was seen that the flutter frequency of the wing was about 30Hz when large deformation was appeared. This type of flutter related to the inside panel vibration mode of the wing. This case was consistent with that of the calculation.

It was seen from calculations that the panel inside mode of the wing was involved in the flutter only the geometric nonlinear condition of the large deformation was considered. Flutter boundary of the wind tunnel model improved obviously at the zero lift angle of attack -2°, so there was not captured with flutter due to limitation of the wind tunnel. It was also consistent with the calculation.

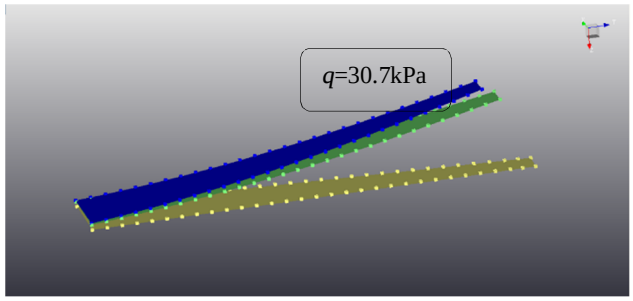

Fig.16 α=-1°, *M*=0.6, deformation test.

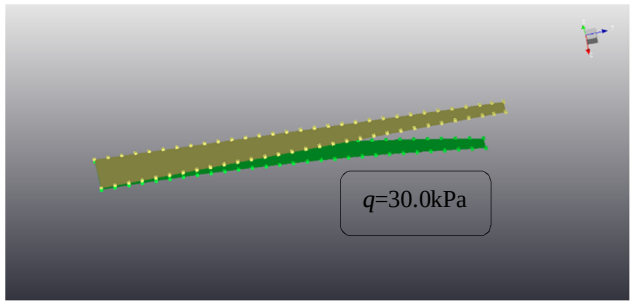

Fig.17 α=-4°, *M*=0.6, deformation test.

Table 2 Flutter testing results

α(°)	*Ma*	q_{cr}	f_{cr}(Hz)
-4	0.6	31.7	29.02
-3		35.70	29.27
-2		>>45.48	—
-1		33.09	33.5

It was most significant that the present wind tunnel experiments verify nonlinear flutter phenomenon of high-aspect-ratio wing model. Also some experimental results can be adopted for verification of related numerical methods.

7 Copyright Issues

References

[1] Lu Z, Cui Y, Schneider D, et al. Aeroelastic responses identification of a high-aspect-ratio flexible wing model and its active flutter suppression strategy. *Aiaa Science and Technology Forum and Exposition*, 2015, AIAA 2016-1226.

[2] Hewson W J, Jones D, Gaitonde A, et al. CFD Aerodynamic Models for Separated Flow on High Aspect Ratio Flexible Wings. *Aiaa/asce/ahs/asc Structures, Structural Dynamics and Materials Conference*, 2018, AIAA 2018-1682.

[3] Castellani M, Cooper J E, Lemmens Y. Nonlinear static aeroelasticity of high-aspect-ratio-wing aircraft by finite element and multibody methods. *Journal of Aircraft*, 2016:1-13.

Contact Author Email Address

E-mail: sy_qianwei@139.com